Fusion Engineering and Design 87 (2012) 1570–1575

Contents lists available at SciVerse ScienceDirect

Fusion Engineering and Design

journal homepage: www.elsevier.com/locate/fusengdes

Mitigation of radio frequency sheaths through magnetic field-aligned ICRF antenna design

M.L. Garrett*, S.J. Wukitch

Plasma Science and Fusion Center, Massachusetts Institute of Technology, Cambridge, MA, USA

ARTICLE INFO

Article history:
Received 10 January 2012
Received in revised form 5 April 2012
Accepted 6 April 2012
Available online 17 May 2012

PACS:
52.25.Vy
52.40.Fd
52.50.Qt
52.55.Fa
52.40.Kh

Keywords:
Alcator C-Mod
ICRF
RF sheath

ABSTRACT

One of the primary challenges of auxiliary heating of tokamaks in the ion cyclotron range of frequencies (ICRF) is the reduction of impurities associated with ICRF operation. On Alcator C-Mod, a new magnetic field-aligned antenna was optimized for magnetic flux coupling, power handling, and minimized integrated parallel electric field ($E_{\parallel}$). Initial simulations performed using both slab and cylindrical geometry suggested nearly complete cancellation of $E_{\parallel}$ in front of the antenna structure for certain toroidal phasings. Using toroidal models, the cancellation of $E_{\parallel}$ is more modest, suggesting 3-D geometrical effects are important. Using finite element method simulations with a 3-D toroidal cold plasma model, multiple antenna phases were analyzed: $[0, \pi, 0, \pi]$, $[0, 0, \pi, \pi]$, $[0, \pi, \pi, 0]$, [0, 0, 0, 0], $[0, \pi/6, 0, \pi/6]$, and $[0, \pi/2, \pi, 3\pi/2]$. In each case, the field-aligned antenna had reduced integrated $E_{\parallel}$ relative to the existing non-aligned antenna geometry, with the greatest reduction for monopole [0, 0, 0, 0] phasing.

1. Introduction

In ITER and in eventual reactors, enhanced impurity confinement due to internal transport barriers (ITBs) and H-mode operation establishes a very low tolerance for high-Z impurities [1]. Experiments have shown that impurity accumulation increases as ICRF power is increased [2]. As a result, one of the primary challenges of ion cyclotron range of frequencies (ICRF) heating is the reduction or elimination of impurity contamination during ICRF operation, particularly for tokamaks with high-Z plasma facing components (PFCs).

Electromagnetic waves in the ion cyclotron range of frequencies are used to provide bulk auxiliary plasma heating in Alcator C-Mod [3] (major radius $R_0 = 0.67$ m, minor radius $a = 0.22$ m). The C-Mod ICRF antennas typically operate at power densities of ~ 10 MW/m^2, approximately 50% higher than is expected in ITER [4]. Similar to ITER, ICRF waves are typically absorbed in a single pass in C-Mod. In addition, C-Mod experiments utilize high-Z PFCs, and contain plasmas where the scrape-off layer (SOL) is opaque to neutrals [5].

Several methods have been proposed to reduce ICRF-specific impurity characteristics: low-Z PFC coatings such as boronization [6]; toroidal phasing of antenna straps [7]; and alignment of Faraday screen elements with the total magnetic field [8], including antenna rotation [9]. On Alcator C-Mod we have designed a new magnetic field-aligned ICRF antenna to minimize ICRF-specific impurity characteristics. A computer-aided design (CAD) drawing of the antenna is shown in Fig. 1, where the back plate is approximately 1.0 m wide and 0.63 m tall.

This article is organized as follows. In Section 2 we examine the correlation between observed impurity characteristics, radio frequency (RF) sheaths and the parallel component of the RF electric field. Section 3 describes the simulation model and method used to characterize the field-aligned antenna. Simulation results are shown in Section 4, followed by conclusions in Section 5.

2. Motivation

Plasma impurities associated with ICRF auxiliary heating are universally observed [7,9–11]. However, the underlying physics of ICRF-specific impurity generation is not well understood, and observations of impurity characteristics differ among various tokamak experiments. On Alcator C-Mod, data suggest that although some impurities originate locally at the ICRF antenna, the primary impurity source is thought to be the outer divertor [12,13]. ASDEX Upgrade data indicate that the ICRF antenna limiters are the primary impurity source [14]. Additionally, JET results suggest that the

* Corresponding author. Tel.: +1 310 907 6556.
E-mail address: mike_g@mit.edu (M.L. Garrett).

0920-3796/$ – see front matter
http://dx.doi.org/10.1016/j.fusengdes.2012.04.011

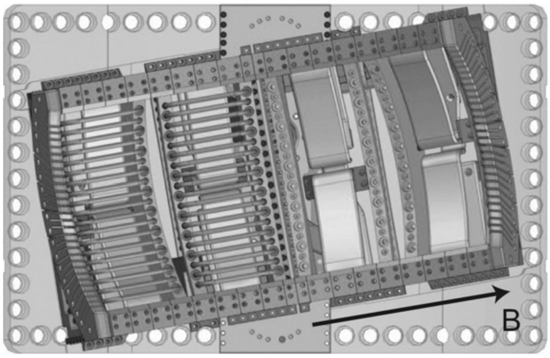

Fig. 1. The new Alcator C-Mod field-aligned ICRF antenna is rotated 10 degrees from horizontal to align with the total magnetic field.

Faraday screens are responsible for most of the observed impurities [15].

Generally, the observed increase in impurities is attributed to either a source mechanism, a transport mechanism, or both [16]. In the first hypothesis, impurities are generated by sputtering of PFCs by energetic ions [17]. In the second case, spatial variation of plasma potentials in front of the antenna establishes local $\mathbf{E}\times\mathbf{B}$ drifts that affect edge transport via the formation of convective cells [18,19]. In each case, the mechanism ultimately responsible for the increase in observed impurities is related to radio frequency (RF) sheath formation [2]. These RF-rectification-enhanced sheaths form on open field lines, which terminate on PFCs and establish sheath potentials significantly higher than those formed across electrostatic sheaths ($V_{SH} \gg 3k_B T_e$). Radio frequency sheaths arise from the nonlinear current response of the plasma to an applied voltage due to the high electron mobility compared to ions along the total magnetic field. As a result, a DC voltage forms along the magnetic field in response to an applied RF field to maintain ambipolarity. According to the model, the primary driving mechanism for these sheaths is the RF electric field component parallel to the equilibrium magnetic field [17]:

$$E_{\parallel} = \frac{\boldsymbol{E}_{\mathrm{RF}} \cdot \boldsymbol{B}}{|B|}. \tag{1}$$

Toroidal phasing of straps on ICRF antennas has a measurable effect on RF sheath potentials and observed impurity production [20,21,8]. Typically, ICRF antennas are operated in dipole phasing $[0, \pi, 0, \pi]$ due to the deleterious effects observed during monopole phasing $[0, 0, 0, 0]$ operation. These effects include increased plasma impurity content [7,20], hot-spot formation [22], and arcing [23]. The current understanding of this experimental observation is that the cancellation of $E_{\parallel}$ along field lines is greater for dipole phasing than for monopole phasing for antenna structures which are not aligned with the equilibrium magnetic field [8,24].

3. Simulation

3.1. Spatial domain cold plasma model

Full wave codes, which solve Maxwell's equations directly inside a plasma model, are typically implemented in the spectral domain. Spectral solvers such as TORIC [25] and AORSA [26], and hybrid spatial / spectral solvers such as TOPICA [27] have achieved good results simulating ICRF heating in tokamaks. More recently, finite element method (FEM) full wave codes have been successfully implemented entirely in the spatial domain [28,29]. Spatial domain FEM codes have several advantages over spectral solvers for ICRF simulation, including the capability to include complex 3-D antenna structures and SOL details that play an important role

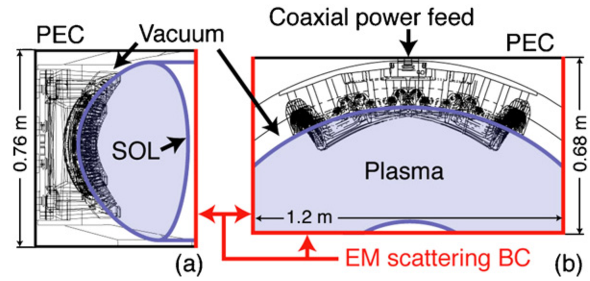

Fig. 2. The simulation domain is shown for the field-aligned antenna in side (a), and top (b) views. An EM wave scattering boundary condition is implemented at the front and sides of the simulation domain to prevent reflection of any waves not damped within the plasma.

in coupling and $E_{\parallel}$ generation. In addition, FEM generally produces numerically sparse matrices, an important consideration for the solution of large electromagnetic problems [30].

For this study, we solve the wave equation for the geometry illustrated in Fig. 2. We have utilized the FEM model described below to solve Maxwell's equations for the electric field $\boldsymbol{E}$, in 3-D toroidal geometry:

$$\nabla \times \nabla \times \boldsymbol{E} = \frac{\omega^2}{c^2} \overleftrightarrow{\boldsymbol{\epsilon}} \cdot \boldsymbol{E} \tag{2}$$

where $\overleftrightarrow{\boldsymbol{\epsilon}}$ is the cold plasma dielectric tensor [31]:

$$\overleftrightarrow{\boldsymbol{\epsilon}} = \begin{bmatrix} S & -iD & 0 \\ iD & S & 0 \\ 0 & 0 & P \end{bmatrix}, \tag{3}$$

with the sum (S), difference(D), and plasma(P) components, given by

$$S = 1 - \sum_j \frac{\omega_{pj}^2}{\omega} \frac{\omega + i\nu_j}{\left(\omega + i\nu_j\right)^2 - \omega_{cj}^2}, \tag{4}$$

$$D = \sum_j \frac{\omega_{pj}^2}{\omega} \frac{\omega_{cj}}{\left(\omega + i\nu_j\right)^2 - \omega_{cj}^2}, \tag{5}$$

$$P = \sum_j \frac{\omega_{pj}^2}{\omega\left(\omega + i\nu_j\right)}. \tag{6}$$

Collisional damping is included by introducing the collision frequency ν_j into the cold plasma two-fluid momentum equations, and ω_{pj}^2, and ω_{cj}^2 represent the plasma and cyclotron frequencies, respectively, for the jth particle species. The dielectric tensor shown in Eq. (3) is rotated to describe an axisymmetric toroidal plasma:

$$\boldsymbol{\epsilon}_{\mathrm{rotated}} = R \cdot \boldsymbol{\epsilon} \cdot R^T, \tag{7}$$

where $R = R_\phi \cdot R_\theta \cdot R_\alpha$, is the rotation matrix used to perform three successive rotations through angles ϕ, θ, and α. These are spatial Euler angles chosen to define a rotation from the Cartesian reference frame to the reference frame of the total magnetic field for each point in the model. This model uses experimental data from Alcator C-Mod. Magnetics data from EFIT [32] are used to reconstruct accurate 3-D magnetic fields in the model. Three dimensional density and temperature profiles are recreated from Alcator C-Mod Thompson scattering data [33]. The SOL is defined by a modified hyperbolic tangent fit of measured density data, shown in Fig. 3. Here, the density profile is artificially truncated at major radius, $R = 90$ cm, to establish a vacuum region in front of the antenna. In addition, detailed 3-D CAD assemblies of the ICRF antenna and vacuum vessel are included in the simulation.